ARTICLE

R. Dean Astumian · Imre Derényi

Fluctuation driven transport and models of molecular motors and pumps

Abstract Non-equilibrium fluctuations can drive vectorial transport along an anisotropic structure in an isothermal medium by biasing the effect of thermal noise ($k_B T$). Mechanisms based on this principle are often called Brownian ratchets and have been invoked as a possible explanation for the operation of biomolecular motors and pumps. We discuss the thermodynamics and kinetics for the operation of microscopic ratchet motors under conditions relevant to biology, showing how energy provided by external fluctuations or a non-equilibrium chemical reaction can cause unidirectional motion or uphill pumping of a substance. Our analysis suggests that molecular pumps such as Na,K-ATPase and molecular motors such as kinesin and myosin may share a common underlying mechanism.

Key words Free energy transduction · Molecular motors · Ion pumps · Ratchets · Maxwells demon

Introduction

We normally think of vectorial motion as arising from macroscopic forces that provide directionality, such as an object falling in a gravitational field, or migration of charged proteins in an applied electric field. Recent work has shown theoretically (Astumian and Bier 1994; Astumian 1997; Hanggi and Bartusek 1996; Magnasco 1993; Prost et al. 1994) and experimentally (Rousselet et al. 1994) that external random fluctuations acting on a particle in an anisotropic medium can cause unidirectional motion in an isothermal medium without a macroscopic force or spatial chemical gradient. Earlier analogous work from a chemical kinetic perspective established that fluctuations of rate constants in a catalyzed chemical reaction can drive the reaction to proceed unidirectionally even if the affinity of the reaction (the

R. D. Astumian (✉) · I. Derényi
Departments of Surgery and of Biochemistry
and Molecular Biology, University of Chicago,
MC 6035, Chicago, IL 60637, USA
e-mail: dastumia@surgery.bsd.uchicago.edu

chemical force) is zero at every instant (Tsong and Astumian 1986; Astumian et al. 1987, 1989; Astumian and Robertson 1993). These results are counterintuitive since random fluctuations in most cases destroy rather than create ordered behavior. In fact it might seem at first glance that fluctuation induced directed motion is contrary to the second law of thermodynamics and could be used to create a perpetual motion machine. Showing in detail why this is not the case strongly motivates the development of rigorous models that can be understood at the level of basic physics.

Aside from theoretical interest, ratchet models share many features with the motion of biomolecular motors such as kinesin (Svoboda et al. 1993) and myosin (Finer et al. 1994), and ion pumps such as Na,K ATPase and Ca ATPase (Lauger 1991) (see Fig. 1). These molecules also bring about net motion without a macroscopic force. The energy for driving flow comes typically from hydrolysis of ATP, but how this chemical reaction defines a preferred direction of motion is far from clear. Recent experiments have demonstrated that, consistent with a ratchet mechanism (Tsong and Astumian 1986; Westerhoff et al. 1986; Astumian et al. 1987), external oscillating (Serpersu and Tsong 1984; Liu et al. 1990) or fluctuating (Xie et al. 1994, 1997) electric fields can drive transport by a molecular ion pump, the Na,K ATPase. Energy from the field substitutes for the energy normally provided by ATP hydrolysis even though the average value of the field is zero. Recent models for fluctuation driven transport provide an explicit mechanism for coupling energy from a non-equilibrium chemical reaction to cause local fluctuations similar to those imposed externally to drive unidirectional transport (Tsong and Astumian 1986; Fulinski 1994).

Despite sharing the similar function of using chemical energy to drive vectorial transport, mechanisms of molecular motors and pumps are typically pictured entirely differently. Molecular pumps are most often modeled in terms of chemical kinetics, where ATP energy is used to change the relative affinities of and barrier heights between different binding sites by sequentially favoring different conformational states of the protein as ATP is bound, hydrolyzed, and the products released. The conformational re-

laxation and molecular transport across the membrane are treated as thermally activated steps. As Lauger summarized (Lauger 1991),

"Ion pumps do not function by a power stroke mechanism; instead, pump operation involves transitions between molecular states, each of which is very close to thermal equilibrium with respect to its internal degrees of freedom, even at very large overall driving force."

Models for molecular motors, on the other hand, have focussed on an ATP driven "power stroke" – a viscoelastic relaxation process where the protein starts from a nonequilibrium, "strained" conformation following product release. The subsequent relaxation does not require thermal activation and can be visualized much as the contraction of a stretched rubber band. In describing how the ribosomal protein synthesizing apparatus works as a molecular motor, Cross (1997) writes

"The protein is like a compressed spring that is held against a trigger – ribosome binding releases the trigger and the protein flies open, exerting force and allowing the phosphate that is generated as a result of GTP hydrolysis to exit from the active site."

This point of view is also expressed in a recent review article (Block 1996). In many ways protein motors have been modeled as miniature versions of macroscopic devices, employing springs, cogs, levers, and the like to effect motion and force generation, where the inescapable molecular fluctuations arising from interaction with the medium are viewed as something to be overcome rather than as an essential feature that can be harnessed to allow for regulation of the timing between chemical and mechanical steps.

Experimental evidence strongly supports the idea that the effect of an external fluctuating electric field on membrane transport is due to biasing of thermally activated transitions along the kinetic pathway. It is our hypothesis that a similar mechanism applies for the case of ATP driven transport by molecular motors, although this is not yet proved and much remains to be clarified.

At first it may seem that the mechanism for using chemical energy to allow molecular motors to move over great distances and exert large forces must indeed by fundamentally different from the way that molecular pumps sit in place in a membrane and use energy from ATP hydrolysis to bias the diffusion of small molecules and ions and do work against an electrochemical gradient. However, the physics of motion of small objects in viscous solution shows that these processes may not be as different as our macroscopically based intuition would suggest and that perhaps the function of molecular motors and pumps may be linked by a common mechanism.

We can see this by considering the Reynolds number (Purcell 1977; Vogel 1989; Berg 1983), R, which is the ratio of the inertial to the viscous forces acting on a particle with a characteristic size (distance) a moving at velocity v. This dimensionless ratio is given by

$$R = a\,v/\nu \tag{1}$$

where ν is the kinematic viscosity. For water, $\nu \approx 10^{-6}$ m²/sec. The equations of motion for two different objects moving with the same Reynolds number (say a large object moving slowly and a small object moving proportionally more rapidly) are the same although the conversion factors to convert back to laboratory lengths and times of course are in general different. Let us consider the case of a molecular motor and an ion pump.

A motor molecule such as kinesin has a characteristic size of 10^{-8} m, and moves with a velocity approaching 10^{-6} m/sec, giving a Reynolds number of 10^{-8}. An ion pump such as the Na,K ATPase can transport up to 1000 ions per sec ($r_{Na^+} \approx 10^{-10}$ m) across the 10^{-8} m thick bilayer membrane, yielding an approximate velocity of 10^{-5} m/sec as a lower bound, resulting in a Reynolds number of 10^{-9}. We have used only very rough estimates, but the Reynolds numbers for ion pumps and molecular motors are both very small. Inertia is then irrelevant, any description of a protein as a spring that flies open should therefore not be taken literally.

The recent Brownian ratchet models, which stress the role of thermal noise (as did some earlier models (Huxley 1957)), offer a unifying hypothesis for motors and pumps and show that mechanisms for molecular motors in which the conformational change of the protein derives thermal activation are consistent with a process in which a protein is translocated over a large distance (10 nm) in a single step, and can exert a large force (piconewtons). In this paper we will discuss some of the background for fluctuation driven motion and examine several models concerning the role of both equilibrium and non-equilibrium fluctuations in the operation of microscopic machines and the thermodynamic basis of extracting work from non-equilibrium fluctuations.

Thermodynamics of ratchets and rectifiers

Many scientists have considered the problem of fluctuation driven motion, perhaps the first being Maxwell, who proposed a device (often whimsically described as an intelligent being or demon) that could open or close a gate separating two containers of a gas depending on a measurement of the velocity of an oncoming molecule (Leff and Rex 1990). If the demon would open the gate only to fast molecules coming from one side and to slow molecules coming from the other, a thermal gradient would be formed. Subsequent analysis has focussed on understanding the energy required to make, store, and eventually erase the necessary measurements of the molecular velocities. Energy dissipation can arise in any of these processes and the minimum amount of energy dissipated is equal to or greater than the work stored by creation of a thermal gradient (Bennet 1987).

Maxwells Demon requires active acquisition of information for operation. Macroscopic ratchets and rectifiers however convert external zero average fluctuating forces into net motion (current) passively. What happens if such
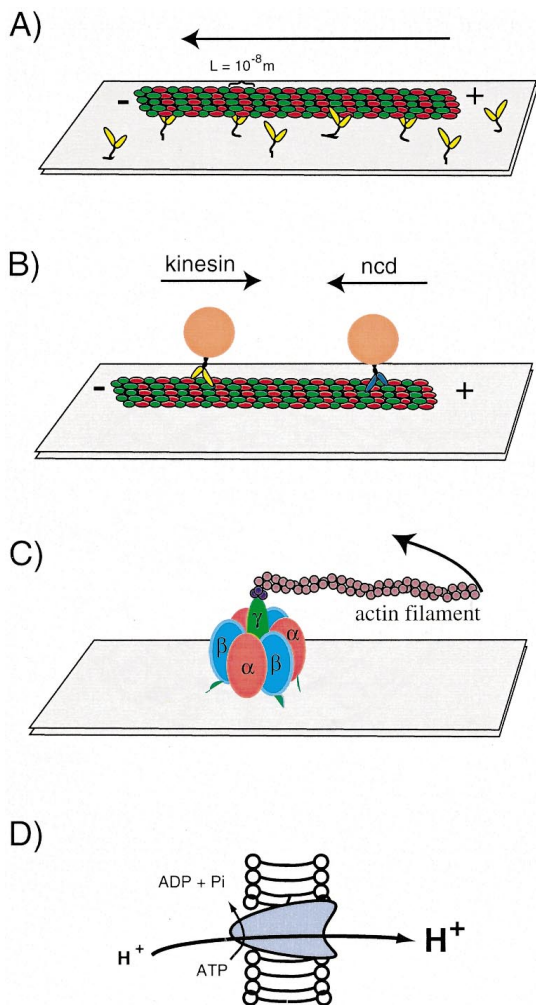
Fig. 1A–D Several molecular motors and pumps, and motility assays. **A** Kinesins immobilized on a glass slide drive the motion of a microtubule in a classic sliding assay (Kron and Spudich 1986). **B** An illustration of recent experiments where low densities of kinesin immobilized on a bead (such that only one kinesin molecule can interact with the microtubule) can drive motion observed by interferometry (Svoboda et al. 1993). The opposite directed motion of a structurally similar Ncd is illustrated, although such an experiment has not been done, and so far there is no evidence that Ncd is processive. **C** Rotational motion of F0F1 ATP-synthase has recently been directly observed (Noji et al. 1997). The F1 subunit was separated and immobilized on a glass slide and an actin filament was attached to its "shaft" to make the ATP hydrolysis driven rotation visible as a circular motion of the actin filament. This was a direct conformation of an early prediction based on symmetry (Boyer 1975). **D** Cartoon of a membrane pump (H$^+$ ATPase) that sits in a membrane, and by ATP dependent conformational changes biases the diffusion across the membrane of ions and small molecules

Fig. 2 Depiction of Feynman's ratchet. Because of the asymmetry of the ratchet's teeth, it might seem that even thermal fluctuations acting on a paddlewheel attached to the ratchet could be used to do work. However, the behavior of the spring is also influenced by collisions with molecules which cause it to vibrate. When the spring is down, molecular collisions with the paddlewheel indeed tend to cause the cog to turn only in the planned direction. However, in the rare event that the spring is up, disengaging the one-way mechanism, the random molecular forces on the paddle cause forward and backward motion with equal probability. It only takes a very tiny movement of the wheel backwards to set the device back one tooth, whereas to send it forward by a tooth requires a much greater motion. If the paddle and the pawl are at the same temperature so that the fluctuations on the pawl are as strong as those driving the paddlewheel, the ratchet, despite appearances will not turn. The equations are approximate formulae for the frequency of moving a step in the clockwise (cw) and counter-clockwise (ccw) direction. $\Delta U = \kappa h^2$ where κ is the spring constant and h is the height of a tooth on the cog

devices are shrunk to microscopic size? This was considered by Smoluchowski (1912), and later by Feynman (1966) with the analysis of a microscopic ratchet (a cog with asymmetric teeth) and pawl (Fig. 2). The ratchet teeth are arranged so that it is impossible to drag the pawl up one face. At first glance it would seem that a paddlewheel attached to such a ratchet should convert thermal fluctuations to unidirectional motion. If the wheel cannot go back-
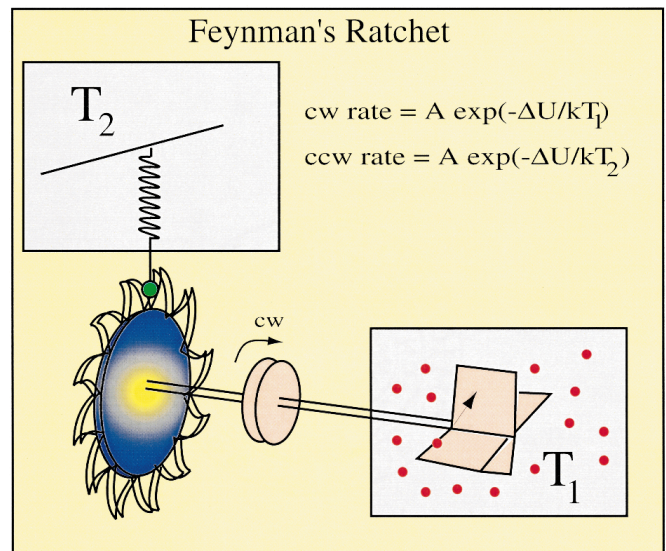
ward, molecules hitting the paddle would cause an irregular but relentless rotation of the wheel that could lift a weight. This would be a perpetual motion machine of the second kind, and a contradiction to the second law of thermodynamics.

Feynman resolved this paradox, showing that consistent application of the laws of statistical mechanics to all parts of the device restores the result that work cannot be extracted from thermal noise in an isothermal system. In order to function, the pawl must be attached to the ratchet by some elastic element, say a spring, which is also influenced by thermal noise. When the pawl is down, the device works as anticipated. However, occasionally the pawl is up, and is disengaged from the ratchet cog. In this rare event, molecular collisions with the paddlewheel cause forward and backward motion with equal probability. Because of the asymmetry, it takes only a tiny motion backward to set the device back by one tooth, but a much larger movement forward to advance the device by one tooth. If the paddlewheel and pawl are at the same temperature, the tendencies to move forward, due to the fluctuating force acting at the paddlewheel, and to move backward due to the fluctuating engagement and disengagement of the pawl,

exactly cancel, and despite appearances, the ratchet will not rotate.

Feynman also considered a modification of this ratchet. The temperature of the pawl and the gas in the box containing the paddlewheel need not be equal. Feynman showed that when the temperatures are different the imbalance in the strength of the thermal noise acting on the paddlewheel and on the spring does indeed cause the cog to rotate. Astonishingly, the device works both ways – when the temperature of the paddlewheel is greater than that of the spring, the ratchet rotates clockwise as our intuition would suggest, but when the temperature of the spring is greater than that of the paddlewheel, the ratchet's rotation is counterclockwise! A simple equation illustrating this can be derived from the two relations for the unidirectional rates shown on Fig. 2, with $T_1 - T_2 = 2 \Delta T$ and $T_1 + T_2 = 2 T$, and $\Delta T \ll T$:

$$\text{net rate} = \frac{A \, \Delta U \, \Delta T}{2 \, k_B T^2} \, e^{-\Delta U / k_B T}, \tag{2}$$

where k_B is Boltzmann's constant. The net rate is nonmonotonic with respect to the average temperature T, and is maximized when $\Delta U = 2 \, k_B T$, illustrating the synergy between "thermal noise" and an external energy supply (the thermal gradient in this case) for doing work.

At first it might seem that Feynman's ratchet, while a useful illustration of the Second Law of Thermodynamics, is not relevant for biological systems since large thermal gradients are not present in organisms (but see (Vale and Oosawa 1990) for a different point of view). But the crucial element is not so much the temperature gradient, but the fact that the system is taken out of equilibrium. It is this departure from equilibrium, coupled with thermal noise, that allows directed motion. Recent work has been devoted to understanding how a chemical reaction can drive motion along a ratchet.

A chemically driven Brownian motor

Consider the one dimensional motion of a charged particle along a periodic lattice of dipoles arranged head to tail (Fig. 3), and let the interaction between the particle and lattice be purely electrostatic (Astumian and Bier 1994). The potential energy profile then consists of a periodic series of minima (wells) and maxima (barriers). For simplicity this can be represented as a sawtooth function. Because of thermal noise, the particle undergoes Brownian motion. Occasionally, it will have enough energy to pass over one of the two barriers surrounding the well in which it starts and move to the well on the right or on the left. It can easily be shown that, despite the anisotropy, without an energy supply the two probabilities are exactly equal.

Now, imagine that this particle catalyzes a chemical reaction, $HS \rightleftharpoons H^+ + S^-$. Because the product molecules H^+ and S^- are charged, the amplitude of the interaction potential between the particle and the dipole lattice depends on whether H^+ or S^- are bound to the particle, resulting in a

coupling between the chemical reaction and the diffusion of the particle along the dipole lattice. The reaction diffusion equations describing this coupled motion are

$$\frac{\partial P_i(x,t)}{\partial t} = \frac{\partial}{\partial x} \left[\frac{U_i'(x)}{\gamma} P_i(x,t) \right] + D \frac{\partial^2 P_i(x,t)}{\partial x^2} \tag{3}$$

$$+ \sum_{j=1}^{3} \left[k_{ji} P_j(x,t) - k_{ij} P_i(x,t) \right], \quad i = 1, 2, 3$$

where $P_i(x,t)$ is the probability density at position x at time t in chemical state i, $U_i'(x)$ is the derivative of the potential at x in state i, γ is the coefficient of viscous friction and is related to the diffusion coefficient D through the fluctuation dissipation relation $D = k_B T / \gamma$, and the k_{ij} are the chemical rate coefficients. At steady state, $\partial P_i(x,t)/\partial t = 0$, and the average velocity of the particle is

$$\langle v \rangle = L \sum_{i=1}^{3} \left[-\frac{U_i'(x)}{\gamma} - D \frac{\partial}{\partial x} \right] P_i(x,t) \tag{4}$$

evaluated at any x, where L is the length of a period. Because of the charge on H^+ and S^-, their local concentrations vary as a function of position along the axis of the dipole lattice ($[H^+]$ is larger near the negative end of the dipole than near the positive end, and the opposite is true for $[S^-]$). Because the radii of the ions H^+ and S^- are very small compared to the radius of the particle their local concentrations equilibrate very fast, and so $[S^-] = [S^-]_{bulk} \exp[-U(x)/k_B T]$ and $[H^+] = [H^+]_{bulk} \exp[+U(x)/k_B T]$ where the subscript bulk denotes the concentration far from the surface of the dipole lattice. For the specific mechanism shown in Fig. 3, k_{21}, k_{23}, and k_{31}, are first-order rate constants and do not depend on the position along the dipole, and $k_{12} = k_{12}^*[SH]$, $k_{13} = k_{13}^*[H^+]$, and $k_{32} = k_{32}^*[S^-]$ are pseudo-first-order rate coefficients into which the concentrations of the reactants have been incorporated. Because $[H^+]$ and $[S^-]$ depend on the position x along the dipole lattice, the rate coefficients k_{13} and k_{32} also depend on the position.

If the chemical reaction is at equilibrium, a direct transition from the uncharged state $i = 3$ to the charged state $i = 2$ is more likely near the positive end of the dipole, where $[S^-]$ is relatively high, than near the negative end of the dipole, where $[S^-]$ is relatively low. Similarly, direct transition from the charged state $i = 1$ to the uncharged state $i = 3$ is more likely near the negative end of the dipole where $[H^+]$ is relatively high than near the positive end of the dipole, where $[H^+]$ is relatively low. The net effect is that transitions from the charged to the uncharged state are more likely near the negative end of the dipole, and transitions from the uncharged to charged state are more likely near the positive end of the dipole. In this case (and in the absence of an external force), the probability density is distributed according to a Boltzmann distribution everywhere and the average velocity of the particle is zero.

If the chemical reaction is away from equilibrium, this relation between the position of the particle and transition probabilities does not necessarily hold. In the extreme case
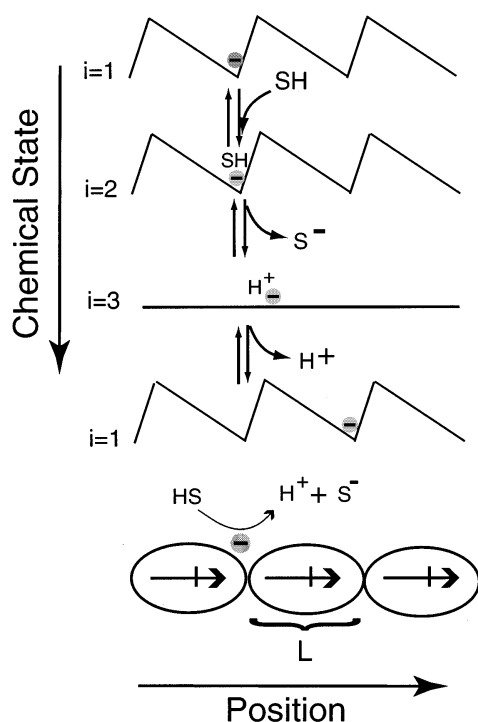
Fig. 3 A chemically driven Brownian motor consisting of an electrically charged catalytic particle undergoing one-dimensional diffusion along a linear polymer of electric dipoles. As the particle catalyzes the chemical reaction $SH \rightleftharpoons S^- + H^+$, its net charge fluctuates depending on its chemical state (i.e., to what it is bound), and so the interaction with the dipole fluctuates. In states 1 and 2, the particle is negatively charged and so is pinned in the region near the positive end of a dipole. When the particle is bound to proton (state 3), the net charge is zero and the particle is free to diffuse along the backbone of the dipole with equal probability to the left and right. Because of the asymmetry of the dipole potential, a short excursion to the right results in the particle being trapped one step to the right when proton dissociates. A much longer and less probable excursion to the left is necessary to trap the particle a step to the left when proton dissociates. Thus it might seem that the charge fluctuations caused by the chemical reaction could drive net motion even when the reaction is at equilibrium. Just as in Feynman's ratchet a more careful consideration as explained in the text shows that this is not true. However, when the reaction is away from equilibrium, directed motion does occur. For $L = 10^{-8}$ m, $\gamma = 2 \times 10^{-8}$ N sec/m and reasonable values of the rate coefficients (Astumian 1997), the calculated average velocity was greater than 3 μm/sec with $\Delta G \approx 1$ kJ/mole

that $[H^+] = [S^-] = 0$, direct transitions from state 1 to state 3, and from state 3 to state 2 cannot occur at all. None of the rate coefficients for the remaining transitions depend on the position of the particle, and so the probability for a transition from the charged to the uncharged state is independent of the position along the axis of the dipole lattice, as is the probability for a transition from the uncharged to the charged state. When during the catalytic cycle, the particle is uncharged (chemical state 3) it can diffuse with equal probability to the left or right. However, a very short excursion to the right brings the particle to a position where dissociation of a proton would cause the particle to be trapped in the well one period to the right of its starting position. A much longer (and hence less probable) excursion to the left would be required to trap the particle in the well one period to the left of the starting point, so net motion to the right is caused by the thermodynamically downhill catalysis.

Thus, we have a rudimentary motor driven by a chemical reaction (Astumian 1997). The mechanism shown in Fig. 3 is obviously a tremendous oversimplification as a description of any actual molecular motor. The interaction between the motor and dipole lattice, and the effect of the catalyzed reaction, were assumed to be purely electrostatic, and the resulting periodic potential was grossly simplified. Nevertheless, with reasonable values of the rate constants and other parameters the motor moves pretty well, with a maximal velocity of several micrometers per second. The stoichiometry is poor – it takes more than 3 HS molecules on average to cause a single step (displacement by a period L), and less than 1 pN of applied force stops the motion. What this simplified motor lacks is what a real biomolecular motor can certainly provide – more complex interaction between the motor and track provided by conformational flexibility, and better regulated coupling between chemical and mechanical events possibly provided by allosteric interaction between the motor and track. However, it seems that many mechanisms may share three characteristic features: (i) Thermal noise to cause Brownian motion or activated transitions from one chemical state to another; (ii) anisotropy arising from the structure of the medium in which the particle diffuses; and (iii) energy supplied either by an external variation of the constraints on the system or by a non-equilibrium chemical reaction.

Brownian ratchets and ion pumps

Perhaps the strongest direct evidence for a ratchet mechanism for free energy transduction by a biomolecule comes from recent experiments showing that the Na,K-ATPase, a biomolecular ion pump can use an external oscillating (Liu et al. 1990) or randomly fluctuating (Xie et al. 1994, 1997) electric field to drive unidirectional transport.

Much work has been done on characterization of the Na,K-ATPase pump (Skou 1957; Lauger 1991). This enzyme is found in almost all mammalian cells, and is important in the maintenance of the osmotic balance of cells, and for using the metabolic energy of ATP hydrolysis to form the Na and K ion gradients rapidly depleted during the action potential in excitable cells. Much of the modeling of the data has revolved around refinement of a kinetic mechanism first proposed by Albers (1967) and Post (1989). The essential feature of this mechanism is the idea that the pump can assume two principal conformations, E_1 (with inward facing ion binding sites) and E_2 (with outward facing ion binding sites). E_1 has a high affinity for Na$^+$ and/or ATP and is stabilized by these ligands, while E_2 has a high affinity for K$^+$ and/or P$_i$ and is stabilized by these ligands. This simple mechanism can account for much of the observed behavior of the ATPase. Recent char-
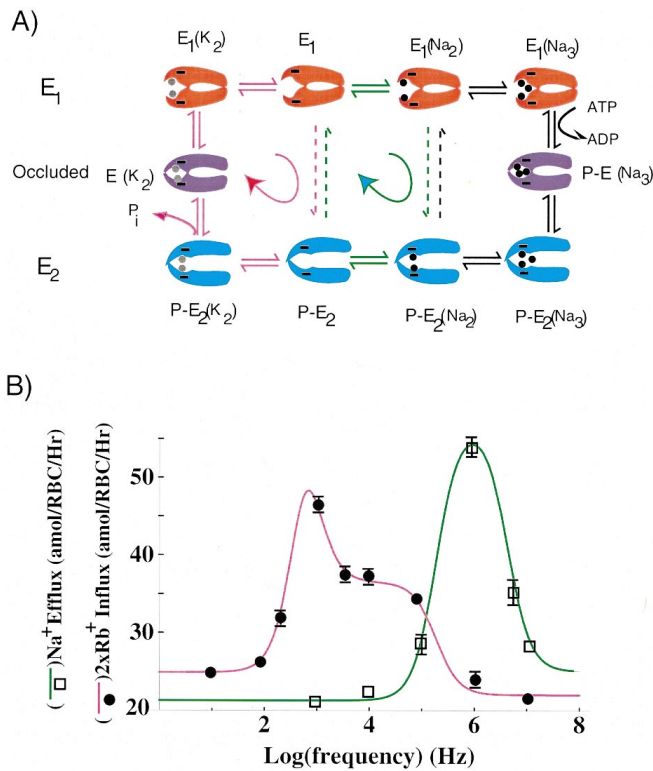
A)

B)

Fig. 4 A Electrostatic model for Na,K-ATPase (Wuddel and Apell 1995). In the ATP driven coupled cycle, the step P-E_2Na$_3$ ⇌ P-E_2Na$_2$ is the most electrogenic, while P-E_2Na$_2$ ⇌ P-E_2 and P-E_2 ⇌ P-E_2K$_2$ are less electrogenic, and E_1 ⇌ E_1K$_2$ and E_1 ⇌ E_1Na$_2$ are not electrogenic, indicating that the access channel for E_2 is more resistive than that for E_1. The transition E_1Na$_2$ ⇌ E_1Na$_3$ is moderately electrogenic, showing that the binding sites for Na are not equivalent. The net transition P-E_2 → P-E_2K$_2$ → E(K$_2$) → E_1K$_2$ → E_1, in which two K are transported across the membrane is also not electrogenic, suggesting that the binding site itself bears charge of –2. The direct transition E_1 ⇌ P-E_2, while not directly accessible to measurement using the technique of Wuddel and Appell, is predicted to be very strongly electrogenic. **B** Data showing the effect of an ac electric field on the ion transport modes of the Na,K-ATPase (Liu et al. 1990) where Rb$^+$ and Na$^+$ transport are induced at different frequencies. The solid lines (magenta for Rb$^+$ and green for Na$^+$) are fits of Lorentzian curves to the data as predicted by a non-linear extension of relaxation kinetic theory (Robertson and Astumian 1991)

A)

B)

Fig. 5 A Cartoon illustration of a protein with two conformational states – one with a high affinity and easy access from the left (exterior), and one with low affinity and easy access from the right (cytoplasm side). Switching between the two conformations is induced by phosphorylation-dephosphorylation of the enzyme. **B** How this can be incorporated into a four state mechanism for active proton transport driven by ATP hydrolysis

acterization of kinetic and equilibrium properties of individual reaction steps has been accomplished using both optical (Rephaeli et al. 1986; Glynn et al. 1987; Steinberg and Karlish 1989) and electrical measurements (Sturmer et al. 1989; Nakao and Gadsby 1986; Rakowski 1993) resulting in the proposal of an electrostatic model of the Na,K-ATPase shown in Fig. 4A (Wuddel and Apell 1995; Rakowski et al. 1997). Additional valuable information on the mechanism of the Na,K-ATPase has been obtained from studying so called non-canonical flux modes, where either Na or K are not added, forcing the pump to proceed via a transition (indicated as dashed arrows) not normally used in the fully coupled mode. The emerging picture of the Na,K-ATPase is of a gated channel-like protein (Hilgemann 1994). The gating is accomplished by phosphorylation dependent conformational changes of the protein, but
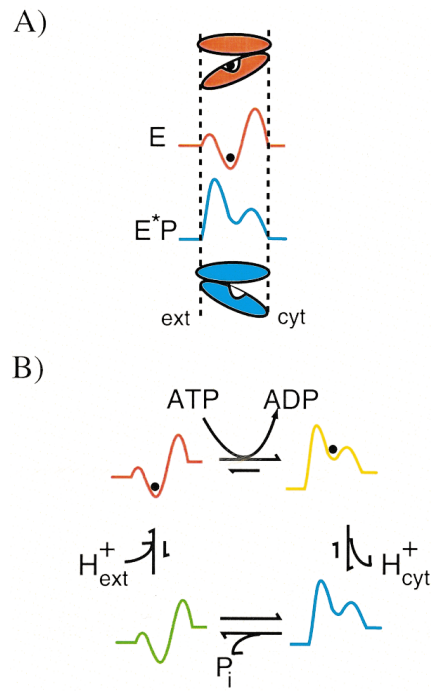
the physical motion of the ion – movement from the bulk to the binding site on one side of the membrane, and dissociation and movement into the bulk on the other side – occurs by diffusion in the presence of the electric field due to charges on the protein.

Because the individual steps of ATP hydrolysis are stochastic, it has long been held that strictly regulated coupling between the chemical events of ATP hydrolysis and mechanical events of ion transport is essential for the function of an ion pump (Jencks 1989). Allosteric interactions between the protein and ligands could ensure that neither ATP hydrolysis nor transport can be completed without the other process occurring, resulting in a strictly ordered sequential kinetic mechanism.

The rigid requirements for such clock-like coupling has recently been challenged by experiments of Tsong and colleagues (Liu et al. 1990; Xie et al. 1994) on Na,K ATPase. In these experiments ATP hydrolysis is suppressed (either by low temperature or by depletion of ATP concentration) and energy for uphill transport provided by externally applied oscillating or fluctuating electric fields. Because the fields are external, there is no mechanism whatsoever for control of the timing of an electric pulse by the occupancy of the ion binding site of the protein. Nevertheless, these external fields are able to drive significant uphill transport. This has been described in terms of a mechanism known as electroconformational coupling (Tsong and Astumian 1986). The key feature of this hypothesis is that the field
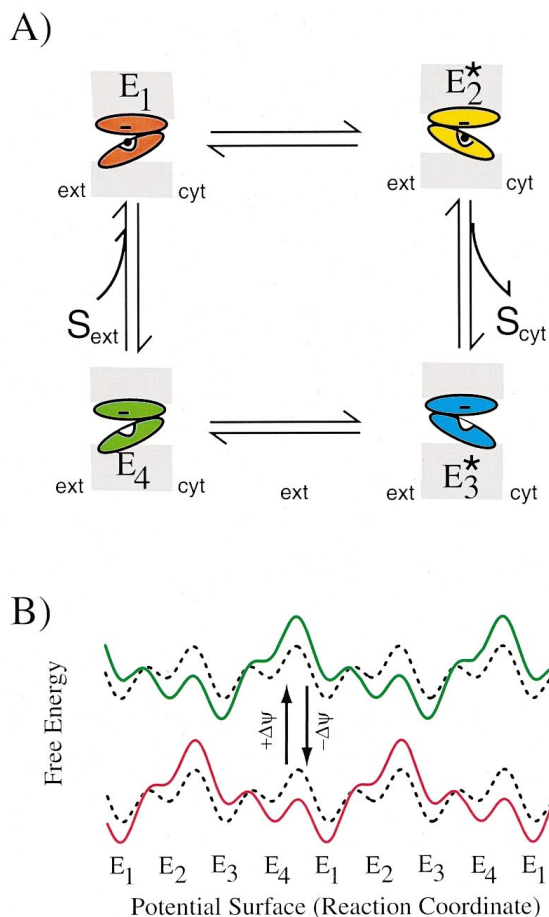
A)

B)

A)

B)

C)

Fig. 6 A Schematic representation of a 4-state model for catalytic transport of an uncharged substance S across a membrane. The conformational transitions $E_1 \rightleftharpoons E_2^*$ and $E_4 \rightleftharpoons E_3^*$ involve a change in the dipole moment of the molecule as well as a change in the exposure of the binding site from the outside to inside facing conformation. The E form has a high affinity for substrate and the E* form has a low affinity. **B** Illustration of an analogy to a pump and dump scheme for optical excitation of a chemical reaction. The dashed line represents the effective one dimensional potential for the reaction at equilibrium in the absence of an applied electric field. The green curve shows the effect of a positive cytosol potential (relative to outside), and the red curve shows the effect of a negative cytosol potential
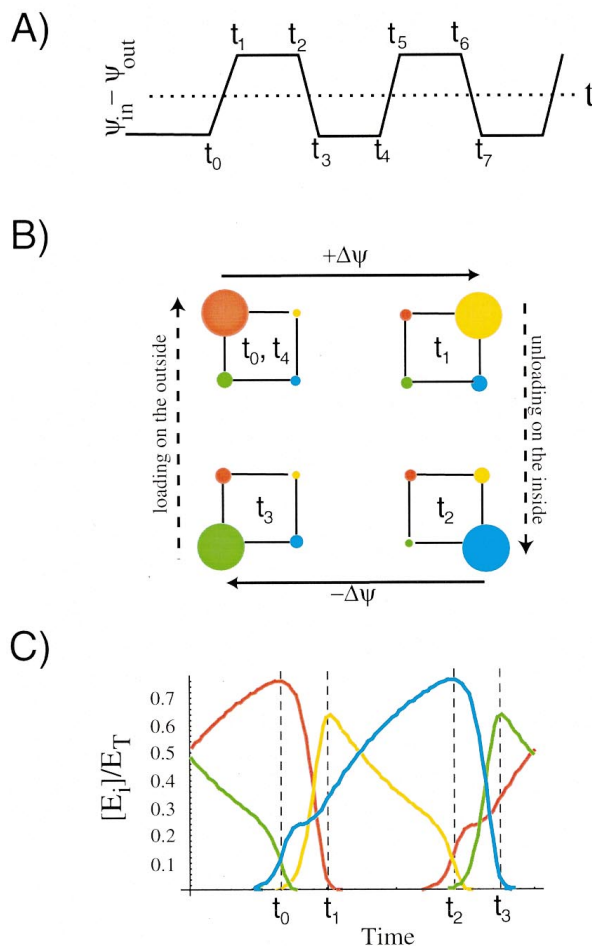
Fig. 7 A The time sequence of a stimulating periodic membrane potential. The time Δt (= $t_1 - t_0 = t_3 - t_2$ etc.) and the time $1/f$ = $t_4 - t_0$. **B** Schematic illustration of the relative state probabilities (E_1 is red, E_2^* is yellow, E_3^* is blue, and E_4 is light green, cf. Fig. 6) at different times during a cycle of the applied field. For $t > t_0$ the enzyme cycle is entrained by the applied field and follows the sequence $E_3^* \rightarrow E_4 \rightarrow E_1 \rightarrow E_2^* \rightarrow E_3^*$ etc., transporting substrate from outside to inside, even against a concentration gradient. **C** Time plots of the enzyme state probabilities as calculated by numerically solving the differential equations describing the kinetics of the system in an oscillating field (Robertson and Astumian 1990)

alters the relative energy levels of the different conformational states of the protein.

The rate of movement of ions across the membrane induced by the ac electric field is independent of ATP concentration but does depend on the frequency ω of the field as shown in Fig. 4B, where the solid lines are the fit curves calculated from an extension of relaxation kinetic theory (Robertson and Astumian 1991) that shows that the flux in general can be expressed as a sum of Lorentzian curves:

$$J_{\text{ion}}(\omega) = \overline{J_\infty} + \sum_{i=1}^{n} \frac{J_i}{1 + \omega^2 \tau_i^2} \tag{5}$$

where the τ_i are the relaxation times and the J_i the relaxation amplitudes of the kinetic system, and $\overline{J_\infty}$ is the flux at a frequency very large compared to any τ_i^{-1}. The effect on

Rb^+ (an analogue of K^+) transport was maximal at 1 kHz, and a maximum effect on Na^+ transport was observed at 1 MHz. The optimal voltage for stimulation in both cases was 20 V/cm. This voltage optimum (not anticipated by the relaxation kinetic approach) may have to do with the field interacting with ion channels and inducing excess noise across the membrane (Fulinski 1994).

The net transport was in the direction stimulated by ATP hydrolysis in vivo in both cases, and from low to high concentration under the experimental conditions. Mechanistically these results can be interpreted in terms of stimulation of non-canonical flux modes of the enzyme, slip cycles that operate when either Na^+ or K^+ are omitted from the medium. The energy from the field drives the "slip" cycles in a direction opposite to that predicted based on the chemical driving force of the cycle. The "slip" transitions

are shown as dashed arrows. The magenta arrows show the most likely cycle stimulated by the ac electric field when Rb^+ is present in the medium, and the green arrows show the cycle most likely stimulated when Na^+ is present. The conformational transition $E_1 \rightleftharpoons P\text{-}E_2$ confers the electrical sensitivity on these processes. Although the charge movement is minimal, the elctric work is $2\,e\,\Delta\psi$ (where "e" is the elementary charge) because the access of the negatively charge binding site is changed from the outside to the cytosol and so the charge effectively moves through the entire membrane potential difference $\Delta\psi$.

How does a zero average electric field cause net transport against an electrochemical gradient? Since the time average of the field is zero, some sort of rectification mechanism must be at work, but the non-monotonic dependence of the transport rate on the frequency of the field suggests a more subtle mechanism than simple rectification of a fluctuating net force or electrochemical gradient. Here, we will discuss one model that is consistent with this observation, and extend the model to suggest how hydrolysis of ATP causes directed transport.

Lauger (1991) has proposed a simple four-state minimal mechanism for a p-type proton ATPase shown in Fig. 5. A key feature is that phosphorylation-dephosphorylation of the enzyme serves to switch the protein between two conformational states. In the phosphorylated state, the enzyme binds a proton tightly, with easy access to the binding site from the outside. In the dephosphorylated state the proton binds much more weakly, and access is easiest from the inside.

The energy dissipated in one cycle of the enzyme comprises three terms: The chemical work done is the ΔG_{ATP} for ATP hydrolysis; since one positive charge is transported per turnover, the electrical work is $+1\,\Delta\psi$; and finally, the concentration work is $k_BT \ln([H^+_{ext}]/[H^+_{cyt}])$.

Clearly, at least one (and most likely several) transition rate constants must depend on the membrane potential. Recent work has suggested that the voltage dependent steps may not be those in which charge translocation occurs, but via the protein conformational change. This is known as an "ion well" mechanism. Consider the case that the binding site in conformation E in Fig. 5A is freely accessible to the solution on the external side. Then the electric potential at that site will be roughly the same as the electrical potential in the bulk exterior. Similarly, if the binding site in the E*P form is freely accessible on the cytosol side, the potential at the binding site will be roughly the same as that in the bulk in the cytosol. Thus, the conformational transition $H\text{-}E \rightarrow H\text{-}E^*P$ will effectively involve moving the charge across the whole membrane potential even though the physical displacement of the charge is minimal.

Because the conformational transitions involve electrical work, a sufficiently large oscillating electric field will cause the conformational state of the transporter to alternate in synchrony with the field. If the affinity for a proton is different in the two states, this electric field induced oscillation can pump the proton against its electrochemical gradient, thereby storing osmotic energy at the expense of energy from the alternating electric field. In Fig. 6 we illustrate this in terms of a four-state mechanism for transport of a substance across a membrane (Astumian 1996). For simplicity, we take the transported substance S to be electrically neutral, and so the overall chemical affinity of the transport reaction is independent of the electric potential difference across the membrane. Even though the overall affinity is independent of the membrane potential difference, the equilibria for some of the individual steps do depend on the membrane potential difference. Because S is uncharged, a DC electric field applied across the membrane will not cause net transport, but the relative concentrations of the transporter states readjust since the different states have different electrical properties. An oscillating or randomly fluctuating electric field however can entrain the cycle and cause uphill pumping as shown in Fig. 7. In order to capture energy from the applied field it is necessary that the affinity for substrate be different for the E and E*. In the example shown in Fig. 7, the affinity of E for S is taken to be much greater than the affinity of E* for S.

There are two relevant time scales: Δt, the time scale for switching the potential difference between + and −; and $1/f$, the inverse of the frequency of oscillation defined by $\Delta\psi(t) = \Delta\psi(t+1/f)$. Since our purpose is to develop an intuitive understanding, consider a limiting case that the time scale for binding substrate is long compared to Δt, but that the time scale for the conformational change between the E states and the E* states is short compared to Δt. Further, let the time scale for binding and debinding of S on either side be short compared to $1/f$, but long compared to Δt, and also that the field amplitude is large.

When the field is made positive on the right, all of the molecules in state E_1 are converted to state E_2^*, and all of the molecules in state E_4 are converted to state E_3^* ($t_0 < t < t_1$). Because the conformational change is fast, this conversion is almost reversible. If the field remains positive on the right for a long time, chemical equilibration between states E_2^*, and E_3^* occurs ($t_1 < t < t_2$). Since the affinity of the E* state for S is small, this means that S is released on the right hand side, and almost all of the transporter molecules end up in state E_3^*. Now, when the field is switched back to become positive on the left hand side, the transporter in state E_3^* is converted to state E_4, and the transporters in state E_2^* are converted to state E_1 ($t_2 < t < t_3$). Shortly after switching the field, state E_4 predominates over state E_1, but the affinity of S for the E form is very large so chemical equilibration between state E_4 and E_1 takes place, resulting in the binding of S on the left hand side ($t_3 < t < t_4$). In Fig. 7C we have plotted the enzyme state probabilities as a function of time. As the field oscillates back and forth, the process continues, with binding of S on the left and release of S on the right, resulting in the eventual formation of a concentration gradient of S. The transport flux at the optimal frequency can be expressed as a generalized Michaelis-Menten equation (Robertson and Astumian 1990). For small fields the cycling continues until the concentration ratio $[S_{cyt}]/[S_{ext}] = \exp[z\,\Delta\psi/k_BT]$ where z is the effective displacement charge associated with the protein conformational transition. For a very large field the effect
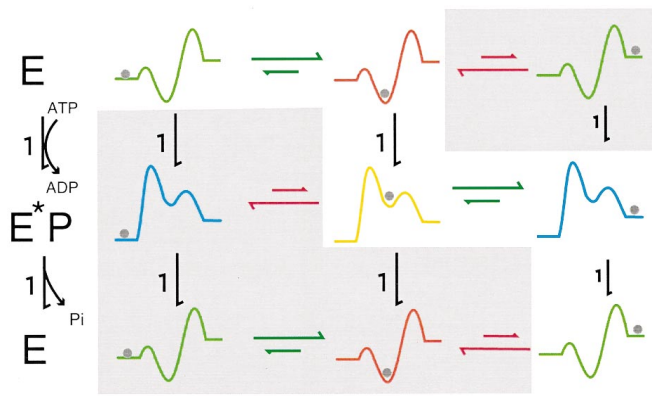
Fig. 8 Illustration of a more general model for the proton transporter in Fig. 5 that includes slip transitions. As explained in the text, the preferred pathway is controlled either by switching the specificity for binding ATP and releasing P_i depending on whether the proton binding site is occupied, or by using differences in the affinities for proton binding in the two states such that the chemical steps are slow compared to thermal activation of proton over the low barriers, but fast compared to thermal activation of proton over the high barriers
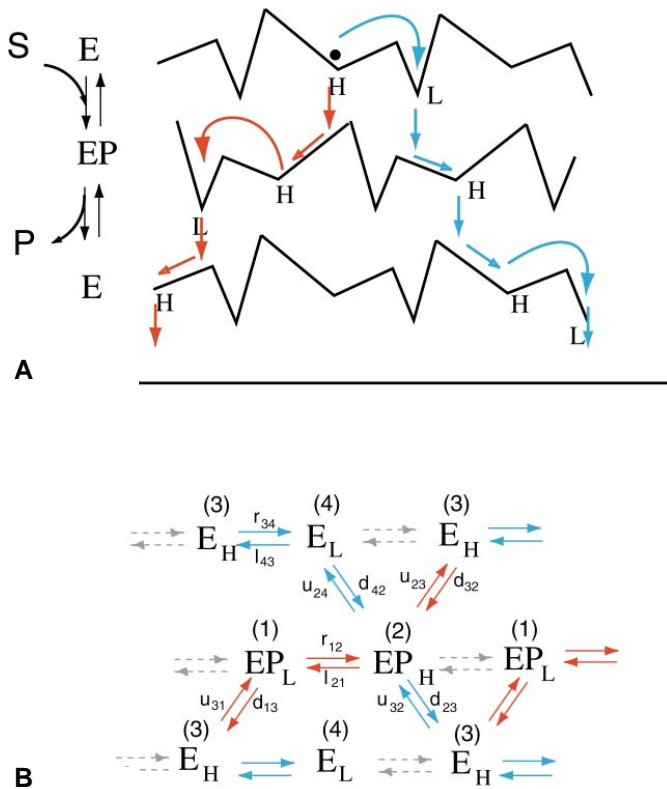

Fig. 10 A Brownian ratchet description of a chemically reversible motor. The direction can be controlled either by the relative rates of S binding and P release, or by the specificity of the H and L states for S and P. The red arrows indicate the path if binding of S is fast and the release of P is slow (or if the H state is specific for binding S and the L state for releasing P), and the blue arrows show the path if binding of S is slow and the release of P is fast (or if the L state is specific for binding S and the H state for releasing P). **B** If the local equilibration within a well is fast, the process can be described in terms of this chemical kinetics mechanism. The rate constants r (l) indicate a step to the right (*left*) and d (u) indicate a step down (*up*), and the subscript ij indicates the starting state (i) and ending state (j). Note: States 1, 2, 3, and 4 correspond to the states of Fig. 6A
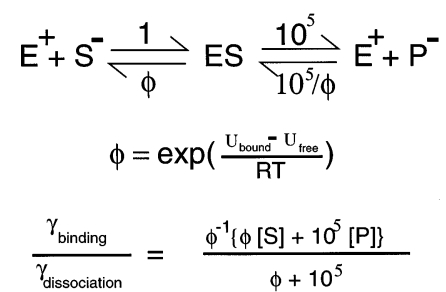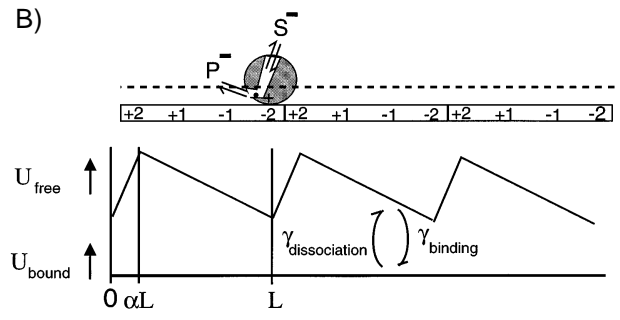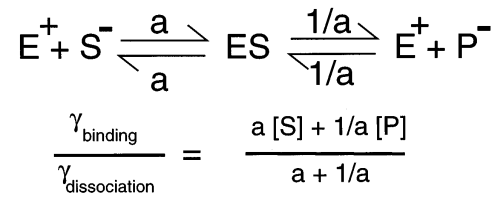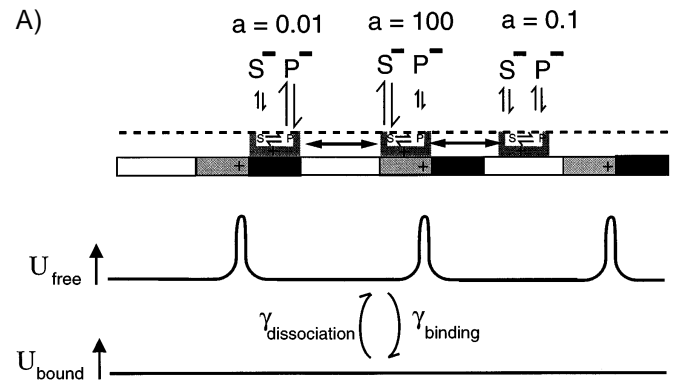

Fig. 9 **A** Schematic illustration of an "information ratchet" in which the anisotropy necessary to break the symmetry of the system and allow net motion is contained within the position dependence of the transition constants between the chemical states. For simplicity we have taken the equilibrium constant for the chemical reaction to be unity, but the results do not depend on this scaling. **B** Illustration of an energy ratchet, where the anisotropy is found in the function describing the potential energy of interaction between the motor and its track. The transition constants can be isotropic. These illustrative examples focus on electrostatic models for simplicity, but the same symmetry and energetic principles could equally well be implemented with models involving conformational change

saturates and cycling continues until the concentration ratio is $[S_{cyt}]/[S_{ext}] = K_{d,cyt}/K_{d,ext}$. The thermodynamic efficiency can approach 100% (Markin et al. 1990).

In order to see the connection between these results and the mechanism of ATP coupled transport, let us reconsider

the proton transporter illustrated in Fig. 5B. The way that we have drawn the mechanism in Fig. 5 implies that proton transport is completely coupled to ATP hydrolysis. This is of course only an approximation, and in principle it is always possible (though perhaps not likely) for a proton to leak across the membrane through the protein without hydrolysis of ATP, or for ATP to be hydrolyzed without pumping a proton. We can see the connection between this type of alternating access model for membrane transport and a Brownian ratchet by rewriting the mechanism in Fig. 5 to explicitly incorporate the possibility of leak, as shown in Fig. 8. Here, we have written all of the chemical transitions along the vertical axis, and the transitions in which a proton moves across the membrane on the horizontal axis. This emphasizes the fact that the two processes are a priori independent, and that coupling is mediated by the conformational switching of the protein between two states with different affinities and access. The mechanism in Fig. 8 is a Brownian ratchet (compare with Fig. 3). The protein conformational changes are driven by ATP hydrolysis, but the transition of the proton from bulk solution to the binding site requires thermal activation over an energy barrier.

The preferred (coupled) pathway is shown as the white zigzag, and follows the same sequence of states as the four state cycle in Fig. 5. In order to achieve tight coupling it is necessary for two "rules" to be followed (Jencks 1989). First, the binding of a proton from the external solution in the E state must be fast compared to the phosphorylation of the enzyme by ATP, and second, the dissociation of a bound proton to the outside must be faster than release of inorganic phosphate in the E*P state.

One way this can be achieved is for the transition between the E and E* states to be slow compared to the hopping of the proton over the low energy barrier, but fast compared to hopping of the proton over the higher barrier. This situation can be achieved only if there is a large difference in proton binding energy (affinity) between the E and E* states. This is what allows an external perturbation to cause directed transport.

If the enzyme is caused by an external field to alternate between the E and E* states sufficiently slowly the system seeks its lowest free energy in each state – proton bound in the E state and proton not bound in the E* state. The most likely path is that which presents the lowest energy barrier – binding from the exterior in the E state and release to the cytosol in the E* state. The net result is that on average, one proton is pumped across the membrane for each cycle of the field if the proton electrochemical gradient is not too big. As the frequency increases, the number of protons pumped per unit time increases. At very large frequencies, however, the conformational transition $E \rightleftharpoons E^*$ cannot keep up and the pumping rate decreases with further increase in the frequency.

A second possibility, open to proteins, is the control of the chemical specificity of the reactions by allosteric interactions between the protein and its ligands. If the protein can be phosphorylated by ATP (or transfer P_i to ADP) only when the proton binding site is occupied, and can be dephosphorylated by transfer of inorganic phosphate to water (or phosphorylated by P_i from water) only when the proton binding site is unoccupied, essentially complete coupling of proton transfer to ATP hydrolysis occurs.

Both of these mechanisms for enforcing a sequential kinetic pathway can be achieved by purely structural features of the enzyme – no continual energy input is required. But these considerations only provide a preferred pathway, and not directionality. If the proton electrochemical gradient would be zero, and the ATP hydrolysis reaction at equilibrium, most of the kinetic traffic would indeed be along the zigzag white path in Fig. 8, but the number of transitions from the upper left corner to the lower right corner would exactly equal the number of transitions from the lower right corner to the upper left corner. The directionality is specified by the signs of the chemical and osmotic free energies – if the ΔG for ATP hydrolysis is greater than the electrochemical potential of proton, there will be more transitions from upper left to lower right, and ATP driven pumping of proton.

Complete coupling occurs when proton association-dissociation to the E state is totally impossible from the inside and to the E* state from the outside, and when the conversion ATP $\rightleftharpoons$ ADP is totally impossible when a proton is not bound to the enzyme, and the conversion E*P $\rightleftharpoons$ E + P_i is totally impossible when a proton is bound. In this case, the net flux is zero only when $\Delta G_{ATP} = \Delta \tilde{u}_{H^+}$, and the efficiency can be 100%, in either direction – uphill transport of a proton driven by hydrolysis of ATP, or synthesis of ATP driven by downhill transport of a proton.

In general, any actual system will have reached a compromise where the enzyme operates at an acceptable rate, but some slip, particularly when doing work against a large load (e.g., pumping against a large $\Delta \tilde{u}_{H^+}$) is allowed. In these realistic situations, the maximal efficiency is less than 100%, and may be different in different directions. Thus, some enzymes may work better using ATP hydrolysis to pump protons uphill, while others may work better using downhill proton transport to synthesize ATP. In order to fully understand the mechanisms of molecular pumps, it is essential to study not only those transitions along the dominant pathway, but also those that result in incomplete coupling and slip.

Biased Brownian motion and molecular motors

The possibility that molecular motors might work by biasing Brownian motion was first proposed by A. F. Huxley (Huxley 1957) in the context of myosin and muscle contraction. His idea is very simple and elegant. The movement of a myosin head relative to the myosin backbone can be modeled as a spring, with different positive or negative displacements representing different conformational states. These states may of course have different chemical properties. Further, the relative affinity of the myosin for actin may depend on the chemical state of the myosin head – a head not bound to ATP may bind to actin with large affin-

ity, while a head bound to ATP may be almost certainly "detached". Consider that a displacement of the spring to the right relative to its equilibrium position corresponds to a conformation from which inorganic phosphate and ADP release is rapid, and a small displacement to the left corresponds to a conformation where ATP binding and hydrolysis is fast. When by thermal diffusion the head has wandered to the right, the myosin head will rapidly dissociate ADP and P_i, grab actin, pull to the left to the equilibrium point, and then rapidly bind ATP and dissociate from actin. The cycle is repeated, hydrolyzing 1 ATP for every incremental displacement of actin to the left. Just as a sanity check, think of the case that ATP hydrolysis is at equilibrium, where by the second law of thermodynamics we know that directed motion is impossible. At equilibrium, the binding of ADP and inorganic phosphate is just as fast as its release for conformations with a displacement to the right, and release of ATP is just as fast as binding of ATP when the myosin head is displaced to the left. In this case, it is easy to show that a displacement of actin to the right is exactly as likely as a displacement to the left.

A key ingredient in this mechanism is that the chemical rates for ATP, ADP, and P_i dissociation and association depend on the position of the myosin head. Recent work has focussed on the possibility that the required anisotropy is built into the interaction between the motor and its track (Astumian and Bier 1996; Julicher et al. 1997). This possibility is conceptually related to Feynman's ratchet discussed earlier, and a specific example is given by the chemical ratchet presented in a previous section.

To better understand this key conceptual difference let us examine two specific simplified models for chemically driven transport – one based loosely on "Maxwell's demon", which we call an information ratchet, and one based on Feynman's ratchet and pawl, which we call an energy ratchet. For simplicity we consider the interaction between the motor and its track in each case to be purely electrostatic.

Information ratchet

In Fig. 9 A we depict a positively charged motor molecule that diffuses along a polymer filament each monomer of which also bears a positive electric charge. The motor is an enzyme that catalyzes the chemical reaction $S \rightleftharpoons P$, where both S and P each bear a negative charge. When the active site on the motor is unoccupied, the net charge on the motor is positive and there is an energy barrier for the motor to pass over the positive charge on the filament backbone, as shown on the curve labelled U_{free}. When the active site is occupied by either S or P the motor is electrically neutral, and in this chemical state there is no barrier for the motor to diffuse over the positive charges on the filament, as reflected in the flat potential energy profile labelled U_{bound}.

If it could be arranged that the active site of the motor would most probably be occupied when the motor is just to the left of a charge on the filament (the gray regions),

and unoccupied when the motor is just to the right of a charge on the filament (the black regions), left to right motion arises trivially. The barriers act as a series of gates. Every time a motor would approach a barrier from the left, S or P would most likely bind causing the "gate" to open. As soon as the motor would cross the threshold, S or P would dissociate, causing the gate to close and preventing backwards diffusion.

This condition is achieved if, for example, the association/dissociation of S is fast and association/dissociation of P is slow in the gray region, and vice-versa in the black region, but only when the $S \rightleftharpoons P$ reaction is far from equilibrium. A simple parametrization in terms of a factor "a" is shown in Fig. 9 A, where in the units used here the dissociation constant $K_{D,S} = K_{D,P} = 1$ for both S and P. Note that the equilibrium constant of the overall reaction is independent of "a" as it must be. The rate at which the system switches from the potential U_{free} to U_{bound} is the sum of the rates for binding S and for binding P, $\gamma_{binding} = \{a[S] + (1/a)[P]\}$. Similarly, the rate at which the potential profile switches from U_{bound} to U_{free} is the sum of the rates for dissociation of S and for dissociation of P, $\gamma_{dissociation} = [a + (1/a)]$.

When the chemical reaction is at equilibrium ([S] = [P]), the ratio $\gamma_{binding}/\gamma_{dissociation}$ is independent of "a", and no directed motion occurs. However, when [S] > 1 > [P], the active site is most likely occupied when $a \gg 1$ (i.e., in the gray region), but most likely unoccupied when $a \ll 1$ (i.e., in the black region). This situation results in net motion from left to right. Note however that an external random switching of the potential from off to on would not generate net motion since there would be no correlation between the position of the motor and the probability for the potential to be on or off.

Energy ratchet

A second possibility for achieving net motion using energy released from a chemical ratchet can be termed an "energy" ratchet. This possibility is illustrated in Fig. 9 B. Once again the motor bears a net charge, but now the filament is modelled as an array of dipoles lined up head to tail. We have shown several charges along the axis of each monomer of the filament so that the motor is never more than a Debye distance (represented by the dashed line) from one of the charges on the filament. When the active site of the motor is unoccupied, the interaction between the charge on the motor and the charges on the dipoles gives rise to a potential energy profile U_{free} that is well approximated by a sawtooth function as shown. When the active site is occupied by either S or P, the charge on the motor is effectively neutralized and the potential energy is approximately independent of position.

Here, the dissociation constants $K_{D,S}$ and $K_{D,P}$ must each depend on position since the difference in electrostatic potential energy between the bound and free states depends on position. In general, this position dependence

is not equally apportioned between the association and dissociation rate constants since the transition state may "look" either more like the free or like the bound state. In Fig. 9 B we have illustrated a specific case loosely inspired by the structure of the myosin molecule (Rayment et al. 1993). In this picture, S enters and leaves the binding cleft from the "top", where we imagine the transition state is at the mouth of the cleft, far from the filament surface. Thus, almost all of the position dependence of $K_{D,S}$ appears in the rate constant for dissociation of S since the transition state looks more like the unbound state. On the other hand, P enters and leaves the binding cleft through an opening that is quite close to the binding site itself, and so the transition state "looks" more like the bound state. Thus almost all of the position dependence of $K_{D,P}$ is expressed in the association rate constant for binding P. At equilibrium, ($[S] = [P]$), a Boltzmann relation between the γ_{binding} and $\gamma_{\text{dissociation}}$ holds and no directed motion occurs (Astumian and Bier 1996). Far from equilibrium however (where $[S] > 10^5 [P]/\phi$), the transitions between "bound" and "free" states are approximately independent of position and directed motion results.

In general, we can write the ratio between the net association and dissociation transition constants in terms of the difference in potential energy levels in the bound and free states of the motor and the free energy of the chemical reaction as

$$\frac{\gamma_{\text{binding}}}{\gamma_{\text{dissociation}}} = C \exp\left(\frac{\Delta U(x)}{k_B T}\right) + g(x)\left[\exp\left(\frac{\Delta G_{\text{chem}}}{k_B T}\right) - 1\right], \tag{6}$$

where C is a constant and $g(x)$ depends on the structure of the motor and track proteins and their interactions with one another and with the substrate and product of the driving chemical reaction. This interaction function is not thermodynamically constrained and can be the target for evolution of motor or pump function.

Note that to achieve a situation sufficiently far from equilibrium with a chemical reaction having an equilibrium constant of one requires an unrealistically large difference in concentration between substrate and product. For a reaction such as ATP hydrolysis however, where the equilibrium constant is very different from 1, concentrations of substrate and product that are more reasonable can provide the same free energy to drive the transport. A membrane potential for a process driven by a proton electrochemical gradient achieves the same result.

Unlike the situation with the information ratchet, for the energy ratchet, applying either a fluctuating macroscopic force, or externally switching the potential off an on *would* drive directed motion, even if the chemical reaction were at equilibrium.

A chemically reversible molecular motor

Several mechanisms for reversing the direction of a Brownian motor by changing the statistical properties of the nonequilibrium fluctuations that power the motion have been given (Bier and Astumian 1996; Chauwin et al. 1995; Tarlie and Astumian 1998). Below, we focus on a chemically driven motor that can be reversed by changing either the rates or specificities on different conformational states for binding substrate and release of product. This model was motivated by consideration of kinesin and Ncd.

Kinesin and Ncd are two members of the kinesin superfamily of microtubule based molecular motors. Powered by ATP hydrolysis these two molecules move in opposite directions along a microtubule – kinesin towards the "+" end and Ncd towards the "–" end. It was hoped that high resolution crystal structures would provide insight into the origins of the directionality. As it turns out however, the two molecules are structurally very similar – almost superposable (Kull et al. 1996; Sablin et al. 1996). Further, they bind with similar orientations on microtubules (Hirose et al. 1996), eliminating the possibility that the opposite directed motion is because the motors bind facing opposite directions. The mystery is deepened by a recent elegant experiment in which a chimera was formed by attaching the motor domain of Ncd to the neck region of *Neurospora* kinesin (Henningsen and Schliwa 1997). Surprisingly, the resulting motor catalyzed "+" end directed motion characteristic of kinesin from which the neck region was taken. Here we present a model based on a "Brownian ratchet" (but incorporating several features of "power stroke" models) in which the direction of motion is controlled by subtle changes of the chemical mechanism of ATP hydrolysis rather than by structural differences in the motor or its interactions with the microtubule.

To approach the detailed mechanism by which chemical energy is used to drive unidirectional motion imagine a particle moving along a filament to which it is associated through Van der Waals and hydrophobic interactions. The particle is an enzyme, and the filament is a long chain of identical protein molecules. Although motion away from the filament is constrained, the particle can still move laterally along the filament by minute conformational changes arising from Brownian motion and accompanied by the breaking and making of many weak contacts. Thus, we can imagine a "detached" state in which the force required to translocate the motor along the axis of the filament is small, but where the force necessary to move the motor perpendicular to the filament is still large.

Typically, there will be a few sites of contact within a periodic unit of the filament where the enzyme will be localized with high probability (binding sites). Occasionally, a transition over an energy barrier to an adjacent binding site on the left or right will occur. The potential energy of the motor along the filament can be drawn as a curve representing the projection of the complex conformational and physical trajectory of the motor molecule onto a single coordinate. This is analogous to collapsing a multidimensional chemical reaction on a single "reaction coordinate". The interpretation of this coordinate must be done with some care. Because of the periodicity, displacement of the enzyme by one period implies that each amino acid of the protein will have been displaced by precisely one period,

and the relationship between the amino acid residues (i.e., the conformation) will be unchanged. Displacement by half a period however does not imply translocation of each amino acid residue of the motor by half a period, and could well involve a significant conformational change.

In Fig. 10 we illustrate a chemically reversible motor, where the interaction between the track and the motor depends on whether the motor is bound to substrate. Within one period there are two binding sites for the protein – a relatively high energy (weak) binding site H, and a relatively low energy (strong) binding site L. Binding substrate to the motor protein changes the locations of these binding sites, as well as the locations of energy barriers between the sites. When the chemical state changes there is first a fast equilibration in the local H binding site of the new chemical state, followed by a slower relaxation from the H site to an L site. When the enzyme is not bound to substrate, a transition from the H to the L site to the right is allowed, while the transition to the L site to the left is blocked by a very high energy barrier. When the enzyme is bound to substrate, a transition from the H to the L site to the left is allowed, while the transition to the L site to the right is blocked. With the setup shown in Fig. 9, the direction of net motion changes when the relative rates for binding of substrate and release of product change.

The blue arrows trace the case for slow association-dissociation of S and fast association-dissociation of P. Because substrate binding is slow, the motor in the unbound state relaxes with high probability to the L binding site to the right before substrate associates. Following substrate association, the motor rapidly equilibrates in the H binding site, but because dissociation of product is fast, P most probably dissociates before relaxation to the L binding site to the left can occur, completing one cycle of chemical reaction S $\rightarrow$ P. This is followed by rapid equilibration in the H binding site, followed by relaxation to the L state before S associates, completing one periodic displacement to the right on the filament.

The red arrows trace the case for rapid association-dissociation of S and slow association-dissociation of P. Here, because substrate binding is fast, the motor in the unbound state does not have time to relax to the L binding site before substrate associates. Following substrate association, the motor rapidly equilibrates in the H binding site, and because dissociation of product is slow, the motor relaxes with high probability to the L binding site before product dissociates. Product dissociation completes a chemical cycle, and the rapid equilibration of the unbound motor in the H site completes one periodic displacement to the left on the filament.

A second way that the direction can be switched is by changing the chemical specificity for the H and L state. It is easy to see that when [S]/[P] > K_{eq}, the motor will move to the right if the L state is specific for binding of S and H state specific for release of P, and to the left if the H state is specific for binding of S and the L state specific for release of P.

If equilibration in the H binding site (well) is fast compared to association-dissociation of S and P, and compared to the relaxation between H and L sites, we can treat the overall process in terms of chemical kinetics, as shown in Fig. 10 B. The rate constants are subject to thermodynamic constraints – any completion of a chemical cycle (conversion of S to P) must reflect the release of the chemical free energy $\Delta G_{chem} = \Delta G^0 + k_B T \ln([S]/[P])$, and any displacement by one period must reflect the mechanical work done in the presence of an external force, $\pm FL$, where L is the period ($\approx 10^{-8}$ m for microtubule), we taken + for a displacement to the right and – for a displacement to the left, and a positive force is directed to the left. These constraints are expressed below:

$$\frac{r_{34}\, d_{42}\, d_{23}}{l_{43}\, u_{24}\, u_{32}} = e^{\frac{\Delta G_{chem}-FL}{k_B T}}, \quad \frac{d_{32}\, l_{21}\, d_{13}}{u_{23}\, r_{12}\, u_{31}} = e^{\frac{\Delta G_{chem}+FL}{k_B T}},$$
$$\frac{d_{32}\, d_{23}}{u_{23}\, u_{32}} = e^{\frac{\Delta G_{chem}}{k_B T}}. \tag{7}$$

One simple set of parameters consistent with these thermodynamic constraints is:

$$
\left|
\begin{array}{llll}
u_{23} = e^{\frac{-F_{ext}L}{4\,k_B T}}\, b/(a\,s) & u_{24} = e^{\frac{+F_{ext}L}{4\,k_B T}}\, b\,s/a & u_{31} = e^{\frac{-F_{ext}L}{4\,k_B T}}\, b\,a/s & u_{32} = e^{\frac{+F_{ext}L}{4\,k_B T}}\, b\,a\,s \\[2mm]
d_{32} = e^{\frac{\Delta G_{chem}}{2\,k_B T}}\, b/(a\,s) & d_{42} = e^{\frac{\Delta G_{chem}}{2\,k_B T}}\, b\,s/a & d_{13} = e^{\frac{\Delta G_{chem}}{2\,k_B T}}\, b\,a/s & d_{23} = e^{\frac{\Delta G_{chem}}{2\,k_B T}}\, b\,a\,s \\[2mm]
r_{12} = e^{\frac{-F_{ext}L}{4\,k_B T}} & r_{34} = K\, e^{\frac{-F_{ext}L}{4\,k_B T}} & l_{21} = K\, e^{\frac{+F_{ext}L}{4\,k_B T}} & l_{43} = e^{\frac{+F_{ext}L}{4\,k_B T}}
\end{array}
\right| \tag{8}
$$

where K is the equilibrium constant for transition from the H to L binding site and b scales the chemical transition rates relative to the mechanical transition rates. The factor a specifies the relative rate for association-dissociation of substrate and product. If $a > 1$, binding and release of product is fast, and that of substrate is slow, and the converse if $a < 1$. The factor s determines the specificity difference – if $s > 1$, the L state is specific for association of substrate, and the H state is specific for dissociation of product. The converse is true if $s < 1$. The assignment of the ΔG_{chem} and external force dependence reflects a minimal chemomechanical coupling (Leibler and Huse 1993; Duke and Leibler 1996) – the effect of the chemical free energy ΔG_{chem} appears only in the transitions in the direction of conversion of S $\rightarrow$ P and the effect of an external force in the transitions in the direction of conversion of P $\rightarrow$ S.

We can separately investigate the two possibilities that the direction is controlled by switching the relative rates

for association-dissociation of S and P, with $s = 1$, or by switching the specificities for binding of S and release of P in the H and L states, with $a = 1$. The kinetic equations for these two cases can be easily derived, and in Fig. 11 A we see the velocity-force curves. In both cases, the relationship is approximately linear, and the velocities and stopping force are in good agreement with values for kinesin in the literature. Figure 11 B shows the efficiency as a function of applied force. We can further investigate the relationship between the parameters by deriving simple analytic equations for the stoichiometry and motor velocity in the absence of an external force, with $s = 1$ and $a \neq 1$

$$\text{Stoich} = \frac{K\,(a^2-1)\,e^{\frac{\Delta G_{\text{chem}}}{2\,k_B T}}\,b}{\left[(K+1)\,a + e^{\frac{\Delta G_{\text{chem}}}{2\,k_B T}}\,b\right]\left[(K+1) + e^{\frac{\Delta G_{\text{chem}}}{2\,k_B T}}\,b\,a\right]}. \quad (9)$$

The stoichiometry is optimized by setting b, the scaling factor for the chemical transitions to $b = (K+1)/e^{\Delta G_{\text{chem}}/(2k_B T)}$, and inserting this into Eq. (9) we find

$$\text{Stoich}_{\text{opt}} = \frac{K\,(a-1)}{(K+1)\,(a+1)}. \quad (10)$$

For $K \gg 1$, the stoichiometry is one step to the right for every chemical cycle when substrate association-dissociation is much faster than product association-dissociation ($a \gg 1$), and one step to the left for every chemical cycle when substrate assocation-dissociation is much slower than product association-dissociation ($a \ll 1$). Using the optimal value for b, we obtain a very simple expression for the motor velocity:

$$v_{\text{mech}} = \frac{a\,(a-1)\left(e^{\frac{\Delta G_{\text{chem}}}{2\,k_B T}} - 1\right) K\,L}{(a+1)\left((a^2+1)\,e^{\frac{\Delta G_{\text{chem}}}{2\,k_B T}} + a\,K\right)}. \quad (11)$$

In the case that the directionality of the motor is controlled by the specificity, s, with $a = 1$ it is easy to see that the stoichiometry approaches 1 (-1) as $s \to \infty$ ($s \to 0$). Thus, the sign of the mechanical flow is positive (negative) if the L (H) state is specific for binding of S and the H (L) state is specific for release of P.

The model in Fig. 10 is a "Brownian Ratchet" even though some of the motion (the downhill slides in Fig. 10 A) has the character of a power stroke. The timing is controlled by thermally activated transitions from the H to L sites, where the H sites act as switching stations at which the chemical rates are compared to the mechanical H → L transition rate. What this simple model shows is that Brownian ratchet mechanisms can have a stoichiometry very close to unity, and that the direction of motion can be controlled by the catalytic reaction rates and specificities even when the interactions between the motor and the microtubule are identical for opposite directed motors in
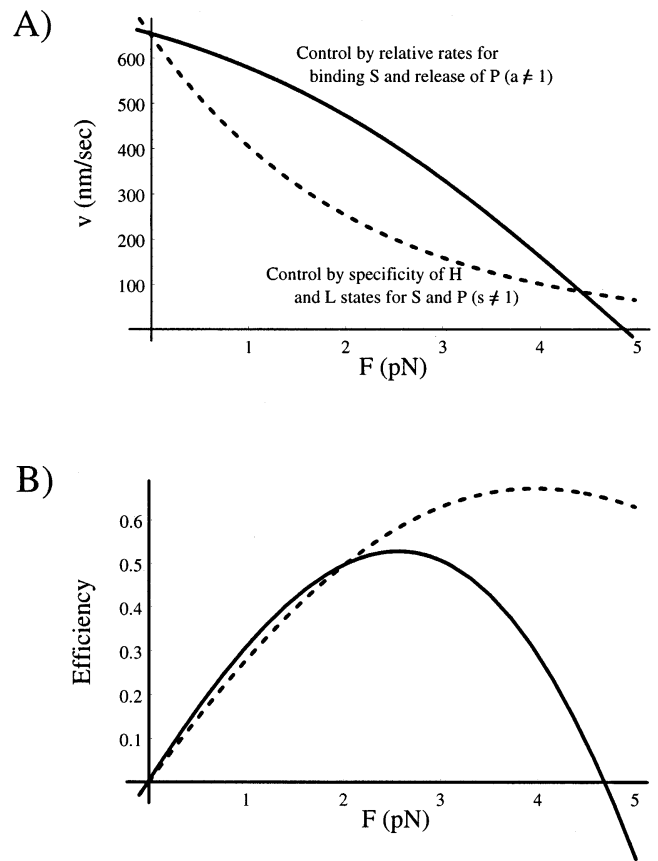

Fig. 11 A Velocity-force curves for the mechanism controlled by relative rates of binding S and releasing P (*solid line*) with $a = 10$, $K = 1000$, and $b = 0.05$/sec which is the optimal value (see text), and for the mechanism controlled by relative specificities of the H and L states for binding S and releasing P (*dashed line*) with $s = 1000$, $K = 650$ and $b = 1$/sec. In both cases, we took $\Delta G_{\text{chem}} = 20\,k_B T$, $T = 300$ K, and $L = 10^{-8}$ m. **B** Plots of the thermodynamic efficiency as a function of force for the two mechanisms, with the same parameters as in **A**. Note that unlike a Carnot engine, the maximal efficiency occurs at a finite velocity

every chemical state. The mechanism discussed here is easily extended to include more realistic double headed models, with both elastic (Derenyi and Vicsek 1996) and chemical (Peskin and Oster 1995) interactions between the heads.

We prefer to imagine the mechanism in terms of a "sliding" motion of the kinesin heads along the microtubule during the mechanical cycle, where the heads neither completely dissociate nor lose energetic contact with their track. In this case, the H and L sites may represent different physical locations along the microtubule.

The mechanism is, however, also in principle consistent with a picture of the heads being completely dissociated during part of the mechanical cycle and held to the microtubule by the other tightly bound head of the dimer. In this case the H and L states represent different conformations of the kinesin head. It is difficult, though, to see how this picture can be consistent with the evidence that single headed kinesins, while not processive (Berliner

et al. 1996), already specify the direction of motion of the motor (Stewart et al. 1993).

Conclusions and perspective

While the past two years have seen an explosion in structural analysis and in techniques for studying single motors and pumps, great challenges remain before a deep understanding of any biomolecular machine is obtained. We predict that paradigms borrowed from basic physics and chemistry will prove useful in the analysis of the molecular events of single motor motion.

One such paradigm is the idea of an activated transition – a process in which thermal energy is borrowed from Brownian noise in the environment to overcome an energy barrier. Such an idea is readily incorporated into the traditional model of a molecular motor in which motion is ascribed to a conformational change called a "power stroke". The insight offered here is that the power stroke may well be a thermally activated transition not unlike the conformational changes by which molecular pumps bias the diffusion of ions to form electrochemical gradients. While many models for molecular motors visualize the motor as completely dissociating from its track before stepping to the next binding site, the model in Fig. 10 suggests that this is not necessary. The process of moving from one binding site to the next may be similar to a one dimensional thermally activated "hopping" process over an energy barrier.

We anticipate that with the ever increasing information on ion pumps and molecular motors it will be possible to develop insight into how each machine works and to establish whether common principles underlie their mechanisms.

References

Albers RW (1967) Biochemical aspects of active transport. Annu Rev Biochem 36: 727–756

Astumian RD (1996) Adiabatic theory for fluctuation-induced transport on a periodic potential. J Phys Chem 49: 19075–19081

Astumian RD (1997) Thermodynamics and kinetics of a Brownian motor. Science 276: 917–922

Astumian RD, Bier M (1994) Fluctuation driven ratchets: molecular motors? Phys Rev Letts 72: 917–922

Astumian RD, Bier M (1996) Mechanochemical coupling of the motion of molecular motors to ATP hydrolysis. Biophys J 70: 689–711

Astumian RD, Robertson B (1989) Nonlinear effect of an oscillating electric field on membrane proteins. J Chem Phys 91: 4891–4899

Astumian RD, Chock PB, Tsong TY, Chen YD, Westerhoff HV (1987) Can free energy be transduced from electric noise? Proc Natl Acad Sci 84: 434–438

Astumian RD, Chock PB, Tsong TY, Westerhoff HV (1989) Effects of oscillations and fluctuations on the dynamics of enzyme catalysis and free-energy transduction. Phys Rev A 39: 6416–6435

Astumian RD, Robertson B (1993) Imposed oscillations of kinetic barriers can cause an enzyme to drive a chemical reaction away from equilibrium. J Am Chem Soc 115: 11063–11068

Bennet C (1987) Demons, engines, and the second law. Sci Am 257: 108–116

Berg HC (1983) Random walks in biology. Princeton University Press, Princeton, NJ

Berliner E, Young EC, Anderson K, Mahatani HK, Gellers J (1996) Failure of a single headed kinesin to track parallel to microtubule protofilaments. Nature 373: 718–721

Bier M, Astumian RD (1996) Biasing Brownian motion in different directions a 3-state fluctuating potential and an application for the separation of small particles. Phys Rev Letts 76: 4277–4280

Block SM (1996) Fifty ways to love your lever: myosin motors. Cell 87: 151–157

Boyer PD (1975) A model for conformational coupling of membrane potential and proton translocation to ATP synthesis and active transport. FEBS Lett 58: 1–6

Chauwin JF, Ajdari A, Prost J (1995) Current reversal in asymmetric pumping. Eur Phys Letts 32: 373–376

Cross RA (1997) A protein-making motor protein. Nature 385: 18–19

Derenyi I, Vicsek T (1996) The kinesin walk: a dynamic model with elastically coupled heads. Proc Natl Acad Sci USA 93: 6775–6779

Duke T, Leibler S (1996) Motor protein mechanics: a stochastic model with minimal mechanochemical coupling. Biophys J 71: 917–922

Kamp F, Astumian RD, Westerhoff HV (1988) Coupling of vectorial proton-flow to a biochemical reaction by localized electric interactions. Proc Natl Acad Sci USA 85: 3792–3796

Faucheaux LP, Bourdieu LS, Kaplan PD, Libchaber A (1995) Optical thermal ratchets. Phys Rev Letts 74: 1504–1507

Feynman RP, Leighton RB, Sands M (1966) The Feynman Lectures on Physics. Addison-Wesley Reading, MA

Finer J, Simmons RM, Spudich JA (1994) Single myosin molecule mechanics: piconewton forces and nanometer steps. Nature 368: 113–119

Fulinski A (1994) Noise-stimulated active transport in biological cell membranes. Physics Letters A 193: 267–273

Glynn IM, Hara Y, Richards DE, Steinberg M (1987) Comparison of rates of cation release and of conformational change in dog kidney Na,K-ATPase. J Physiol (London) 383: 477–485

Hanggi P, Bartussek R (1996) Brownian rectifiers: how to convert Brownian motion into directed transport. In: Parisi J, Muller SC, Zimmerman W (eds) Nonlinear physics of complex systems – current status and future trends. Springer, Berlin Heidelberg New York, pp 1–7

Henningsen U, Schliwa M (1997) Reversal in the direction of movement of a molecular motor. Nature 389: 93–95

Heyse S, Wuddel I, Apell H-J, Sturmer W (1994) Partial reactions of the Na,K-ATPase: determination of rate constants. J Gen Physiol 104: 197–240

Hilgemann DW (1994) Channel-like function of the Na,K pump probed at microsecond resolution in giant membrane patches. Science 263: 1429–1432

Hirose K, Lockhart A, Cross RA, Amos LA (1996) Three dimensional cryoelectron microscopy of dimeric kinesin and ncd motor domains on microtubules. Proc Natl Acad Sci USA 93: 9539–9544

Huxley AF (1957) Muscle structure and theories of contraction. Prog Biophys Biophys Chem 7: 255–318

Jencks WP (1989) Utilization of binding energy and coupling rules for active transport and other coupled vectorial processes. Method Enzymol 171: 145–165

Julicher F, Ajdari A, Prost J (1997) Modeling molecular motors. Rev Mod Phys 69: 1269–1281

Kron SJ, Spudich JA (1986) Fluorescent actin filaments move on myosin fixed to a glass surface. Proc Natl Acad Sci 83: 6272–6276

Kull JF, Sablin EP, Lau R, Fletterick RJ, Vale RD (1996) Crystal structure of the kinesin motor domain reveals a structural similarity to myosin. Nature 380: 550–555

Lauger P (1991) Electrogenic ion pumps. Sinauer, Sunderland, MA

Leff HS, Rex AF (1990) Maxwells demon: entropy, information, computing Princeton University Press, Princeton, NJ

Leibler S, Huse D (1993) Porters vs rowers: a unified stochastic model of motor proteins. J Cell Biol 121: 1357–1368

Liu DS, Astumian RD, Tsong TY (1990) Activation of Na^+ and K^+ pumping mode of (Na,K)-ATPase by an oscillating electric field. J Biol Chem 265: 2760–2767

Magnasco M (1993) Forced thermal ratchets. Phys Rev Letts 67: 1477–1481

Markin VS, Tsong TY, Astumian RD, Robertson B (1990) Energy transduction between a concentration gradient and an alternating electric field. J Chem Phys 93: 5062–5066

Nakao M, Gadsby DC (1986) Voltage dependence of Na translocation by the Na/K pump. Nature 323: 628–630

Noji H, Yasuda R, Yoshida M, Kinosita K (1997) Direct observation of the rotation of F1-ATPase. Nature 386: 299–302

Peskin CS, Oster G (1995) Coordinated hydrolysis explains the mechanical behavior of kinesin. Biophys J 68: 202s–211s

Post RL (1989) Seeds of sodium, potassium ATPase. Annu Rev Physiol 51: 1–15

Prost J, Chawin J-F, Peliti L, Ajdari A (1994) Asymmetric pumping of particles. Phys Rev Letts 72: 2652–2655

Purcell EM (1977) Life at low Reynolds number. Am J Phys 45: 3–11

Rakowski RF (1993) Charge movement by the Na/K pump in Xenopus oocyte. J Gen Physiol 101: 117–144

Rakowski RF, Gadsby DC, De Weer P (1997) Voltage dependence of the Na/K pump. J Membrane Biol 155: 105–112

Rayment I, Holden HM, Whittaker M (1993) Structure of the actin-myosin complex and its implications for muscle contraction. Science 261: 58–65

Rephaeli A, Richards D, Karlish SJD (1986) Conformational transitions in fluorescein-labeled (Na,K)ATPase reconstituted into phospholipid vesicles. J Biol Chem 261: 6248–6254

Robertson B, Astumian RD (1990) Kinetics of a multistate enzyme in a large oscillating field. Biophys J 57: 689–696

Robertson B, Astumian RD (1990) Michaelis-Menten equation for an enzyme in an oscillating electric field. Biophys J 58: 969–974

Robertson B, Astumian RD (1991) Frequency dependence of catalyzed reactions in a weak oscillating field. J Chem Phys 94: 7414–7419

Rousselet J, Salome A, Ajdari A, Prost J (1994) Directional motion of Brownian particles induced by a periodic asymmetric potential. Nature 370: 446–448

Sablin EP, Kull JF, Cooke R, Vale RD, Fletterick RJ (1996) Crystal structure of the motor domain of the kinesin-related motor ncd. Nature 380: 555–559

Serpersu EH, Tsong TY (1984) Activation of electrogenic Rb^+ transport of Na^+K^+ATPase by an electric field. J Biol Chem 259: 7155–7162

Skou JC (1957) The influence of some cations on an adenosine triphosphatase from peripheral nerves. Biochim Biophys Acta 23: 394–401

Smoluchowski M von (1912) Experimentell nachweisbare der üblichen Thermodynamik widersprechende Molekularphänomene. Physik Z 13: 1069–1080

Steinberg M, Karlish SJD (1989) Studies on conformational change sin Na,K-ATPase labeled with 5-iodoactamido-fluorescein. J Biol Chem 264: 2726–2734

Stewart RJ, Thaler JP, Goldstein LSB (1993) Direction of microtubule movement is an intrinsic property of the motor domains of kinesin heavy chain and *Drosophila* ncd protein. Proc Natl Acad Sci USA 90: 5209–5213

Sturmer W, Apell H-J, Wuddel I, Lauger P (1989) Conformational transitions and charge translocation by the Na,K pump: comparison of optical and electrical transients elicited by ATP-concentration jumps. J Membrane Biol 110: 67–86

Svoboda K, Schmidt CF, Schnapp BJ, Block SM (1993) Direct observation of kinesin stepping by optical trapping interferometry. Nature 365: 721–727

Tarlie M, Astumian RD (1998) Optimal modulation of a Brownian ratchet and enhanced sensitivity to an applied force. Proc Natl Acad Sci USA (in press)

Tsong TY, Astumian RD (1986) Absorption and conversion of electric field energy by membrane bound ATPases. Bioelectrochem Bioenerg 15: 457–476

Vale R, Oosawa F (1990) Protein motors and Maxwell's Demon: does mechanochemical transduction involve a thermal ratchet? Adv Biophysics 26: 97–134

Vogel S (1989) Life in moving fluids: the physical biology of flow. Princeton University Press, Princeton, New Jersey

Westerhoff HV, Tsong TY, Chock PB, Chen Y-D, Astumian RD (1986) How an enzyme can capture free energy from an oscillating electric field. Proc Natl Acad Sci USA 83: 4734–4738

Wuddel I, Apell H-J (1995) Electrogenicity of the sodium transport pathway in the Na,K-ATPase probed by charge-pulse experiments. Biophys J 69: 909–921

Xie TD, Marszalek P, Chen Y-D, Tsong TY (1994) Recognition and processing of randomly fluctuating electric signals by Na,K-ATPase. Biophys J 67: 1247–1251

Xie TD, Chen Y, Marszalek P, Tsong TY (1997) Fluctuation-driven directional flow in biochemical cycles: further study of electric activation of Na,K pumps. Biophys J 72: 2495–2502